Supplementary Information (SI) for RSC Sustainability.
This journal is © The Royal Society of Chemistry 2025

Supporting Information

Hierarchically Structured MOF-on-MOF Photocatalysts with Engineered Charge Dynamics for Sustainable Green Fuel Generation

Priyanka Priyadarshini[a], Subrat Kumar Sahoo[a], Kulamani Parida[a]*

[a]Centre for Nano Science and Nano Technology, S 'O' A (Deemed to be University), Bhubaneswar—751 030, Odisha (India)

***Corresponding Author**

kulamaniparida@soauniversity.ac.in & paridakulamani@yahoo.com

1. Chemicals used

Titanium isopropoxide ($Ti(O\text{-}iPr)_4$), 2-amintoterphthalic acid, Cobalt nitrate ($Co(NO_3)_2 \cdot 6H_2O$), 2-methylimidazole, Graphene Oxide, Methanol, Dimethylformamide (DMF), and Isopropanol (IPA) were obtained from Merck and were used without further purification.

2. Characterization details

2.1. Physicochemical characterization techniques

Powder X-ray diffraction (XRD) patterns were recorded on a Rigaku Ultima IV diffractometer employing Cu K_α radiation ($\lambda = 0.154$ nm) at a scan rate of 2^0 min^{-1} to assess the crystalline phases of the samples. The elemental composition was determined by inductively coupled plasma–optical emission spectrometry (ICP-OES) using a PerkinElmer Optima 2100DV system. UV–visible diffuse reflectance spectroscopy (UV–Vis DRS) was performed with a JASCO V-750 spectrophotometer using $BaSO_4$ as a reference to evaluate the optical absorption and estimate the bandgap energy. Photoluminescence (PL) spectra were obtained using a JASCO FP-8300 spectrofluorometer to probe charge carrier recombination behavior. The surface morphology and microstructural features of the photocatalysts were examined by scanning electron microscopy (SEM, ZEISS SUPRA-55) and transmission electron microscopy (TEM, JEOL JEM-2100 operated at 200 kV). X-ray photoelectron spectroscopy (XPS) analysis was carried out on a VG Microtech Multilab ESCA 3000 system equipped with a non-monochromatized Mg K_α source to determine the surface elemental states and chemical compositions. Specific surface area and porosity characteristics were analyzed via N_2 adsorption–desorption isotherms using the Brunauer–Emmett–Teller (BET) method on a Quantachrome NOVA2200e instrument. Wettability was evaluated by static water contact angle measurements using a Kyowa DMe-211 goniometer, with average values calculated from three different positions per sample. Electrochemical characterizations, including linear sweep voltammetry (LSV), Mott–Schottky (MS) analysis, transient photocurrent response, and electrochemical impedance spectroscopy (EIS), were performed using an IVIUM n-STAT multichannel electrochemical workstation in a standard three-electrode configuration comprising a sample-coated FTO working electrode, a platinum wire counter electrode, and an Ag/AgCl reference electrode. Time-resolved photoluminescence (TRPL) spectra were recorded using an Edinburgh FLS90 fluorescence spectrometer coupled with a multichannel scaling (MCS) module and an F290H pulsed xenon microsecond flash lamp as the excitation source.

2.2. Photoelectrochemical characterization process

The photoelectrochemical properties of the synthesized materials were assessed using a three-electrode electrochemical cell equipped with a 300 W Xe light source and a 400 nm cut-on long pass filter. Initially, the FTO substrate was cleaned thoroughly with deionized water and acetone. The conductive surface of the FTO was then uniformly coated using the drop-casting method with a sample paste prepared by mixing 50 mg of the sample with 0.1 mL of ethanol and 300 µL of 1% Nafion, followed by drying under ambient conditions. Linear sweep voltammetry (LSV) measurements were conducted within a potential range of 0 to −1.5 V, while transient photocurrent analysis was carried out for 300 seconds under light exposure at a bias voltage of 0.25V. Mott–Schottky (MS) and electrochemical impedance spectroscopy (EIS) measurements were performed at varying frequencies of 500, 1000, and 1500 Hz for MS, and from 10^5 to 0.1 Hz at zero potential bias for EIS. All experiments were conducted using a 0.1 M Na_2SO_4 electrolyte with a pH of 6.8.

3. Photocatalytic experimental setup

3.1. Photocatalytic H_2O_2 production experiment

The photocatalytic activity of the synthesized materials toward the oxygen reduction reaction (ORR) for H_2O_2 production was evaluated in a quartz-jacketed glass photochemical reactor equipped with a 250 W medium-pressure Hg lamp (410 nm < λ < 700 nm) and a circulating water chiller to maintain the reaction temperature at 25 °C. For each experiment, 0.01 g of photocatalyst was dispersed in 10 mL of deionized water containing 1 mL of 99% isopropanol (IPA), followed by 15 minutes of ultrasonication. The suspension was purged with O_2 for 30 minutes in the dark under gentle stirring to ensure saturation. The mixture was then irradiated under visible light for 2 hours, after which the photocatalyst was separated by centrifugation and filtration (Whatman 41). To the resulting filtrate, 800 µL of 0.1 M KI and 0.01 M $(NH_4)_6Mo_7O_{24}$ were added, and the absorbance of iodine was measured at 350 nm using a UV–vis spectrophotometer after 5 minutes to quantify the H_2O_2 concentration. A control test in the absence of light and catalyst confirmed no H_2O_2 formation. Reactive species trapping experiments were carried out under identical conditions using p-benzoquinone (p-BQ) as a superoxide radical scavenger and dimethyl sulfoxide (DMSO) as a hole scavenger. Furthermore, a nitroblue tetrazolium (NBT) assay was employed to verify superoxide radical generation via absorbance measurements.

3.2. Photocatalytic H_2 evolution experiment

The photocatalytic hydrogen (H_2) generation activity of the synthesized materials was evaluated in a sealed 100 mL quartz batch reactor. For each experiment, 10 mg of photocatalyst was dispersed in 10 mL of an aqueous solution containing 10 vol% methanol, which served as a

sacrificial electron donor. The suspension was continuously stirred using a magnetic stirrer to ensure uniform dispersion and prevent aggregation of photocatalyst particles. Before irradiation, the system was purged with high-purity nitrogen gas for 30 minutes to eliminate dissolved oxygen and establish an inert atmosphere. Photocatalytic reactions were carried out under visible light irradiation using a 125 W medium-pressure mercury lamp, positioned at a fixed distance of 8.7 cm from the reactor. The reaction mixture was irradiated for 1 hour, and the evolved hydrogen was collected via the water displacement method. Quantitative analysis of the generated hydrogen gas was performed using a gas chromatograph (Agilent GC-7890B) equipped with a 5 Å molecular sieve column and a thermal conductivity detector (TCD). Control experiments confirmed that no hydrogen evolution occurred in the absence of light or catalyst, emphasizing the photocatalytic nature of the reaction. The H_2 evolution results for both pristine and composite photocatalysts after 60 minutes of irradiation are presented in Fig. 4(c).

4. Calculation of solar to chemical conversion efficiency (SCC %)

SCC of MNZ towards H_2O_2 generation under 250 W Hg-lamp can be calculated by following the equation below:

$$\textbf{SCC \%} = \frac{\Delta G^{\circ}\, for\ H_2O_2 generation \left(\frac{J}{mol}\right) \times H_2O_2\ produced\ (mol)}{Input\ energy\ (W)\ \times\ reaction\ time\ (s)} \times 100 \quad ..(S1)$$

Further, for H_2O_2 evolution, ΔG° is 117 kJ·mol^{-1}. The irradiance of 250 W Hg-lamp is 1.33 Wcm^{-2} and the irradiated area is 127.17cm^2.

Input Energy (W) = Irradiance (W cm^{-2}) * Irradiated area (cm^2)

= 1.33 * 127.17

= 169.17 W

Putting all these in equation (1), the SCC efficiency is calculated to be 0.025%.

5. Calculation of Apparent Quantum Efficiency (AQE) for H_2O_2 generation

To evaluate the apparent quantum efficiency (AQE) for H_2O_2 generation, the MNZ photocatalyst was tested under monochromatic light irradiation at selected wavelengths (λ = 340, 400, 450, 500, and 550 nm) using appropriate bandpass optical filters. The intensity of the incident light at each wavelength was accurately measured using a calibrated optical power meter. The AQE was then determined using the following equation:

$$\text{AQE} = \frac{2 \times \textit{the number of evolved } H_2O_2 \textit{ molecules}}{\textit{the number of incident photons}} \times 100\% \quad \text{.....(S2)}$$

$$= \frac{Ne}{Np} \times 100\% = \frac{2 \times M \times NA \times h \times c}{S \times P \times t \times \lambda} \times 100\%$$

In this equation, M represents the amount of H_2O_2 produced during the photocatalytic reaction, expressed in moles. N_a is Avogadro's constant (6.023×10^{23} mol^{-1}), h denotes Planck's constant (6.626×10^{-34} J·s), and c is the speed of light in a vacuum (3.0×10^8 m/s). S indicates the irradiated surface area of the photocatalyst, P corresponds to the incident light power, t is the total irradiation time, and λ is the wavelength of the monochromatic light used during the experiment.

6. Calculation of Apparent Conversion Efficiency (ACE) for H_2 Evolution.

$$\text{ACE} = \frac{\textit{Stored chemical energy } (SCE)}{\textit{Incident light intensity } (ILI)} \times 100 \quad \text{.....(S3)}$$

$$= \frac{\textit{moles of } H_2 \textit{ produced } * \Delta Hc}{150\ mW\ cm - 2\ (\textit{spherical surface area on which light falls})} \times 100$$

$$= \frac{5.972 \times 10^{-8} \times 285{,}800\ J/mol}{70\ mWcm^{-2} \times 3.141\ \times 2.25 cm^2} \times 100$$

$$= 3.45\%$$

7. BET Surface Area Analysis

The specific surface areas of MNH, ZIF-67, and MNZ were measured by the Brunauer–Emmett–Teller (BET) method on the basis of nitrogen adsorption–desorption isotherm data measured at 77 K. The BET surface area was estimated from the linear region of the BET plot over the relative pressure range $0.05 \leq \frac{p}{p_0} \leq 0.30$. The BET equation is expressed as:

$$\frac{p}{V_a(p_0 - p)} = \frac{1}{V_m C} + \frac{C - 1}{V_m C} \times \frac{p}{p_0} \quad \text{.....(S4)}$$

Here, V_a is the volume of nitrogen adsorbed at the standard temperature and pressure (STP), V_m is the monolayer adsorption capacity, and C is the BET constant. A linear plot of $\frac{p}{V_a(p_0 - p)}$ versus $\frac{p}{p_0}$, allows the determination of the calculation of Vm from the slope and intercept as:

$$V_m = \frac{1}{Slope + Intercept} \quad \text{.....(S5)}$$

The specific surface area was calculated from V_m according to the equation:

$$A = \frac{V_m \times N \times S}{V} \quad \text{.....(S6)}$$

Where N is Avogadro's number (6.023×10^{23} molecules/mol), S is the adsorption cross-section area of the adsorbing species (0.162 nm^2 for N_2), and V is the molar volume of the gas (22.414 L for an ideal gas at STP).

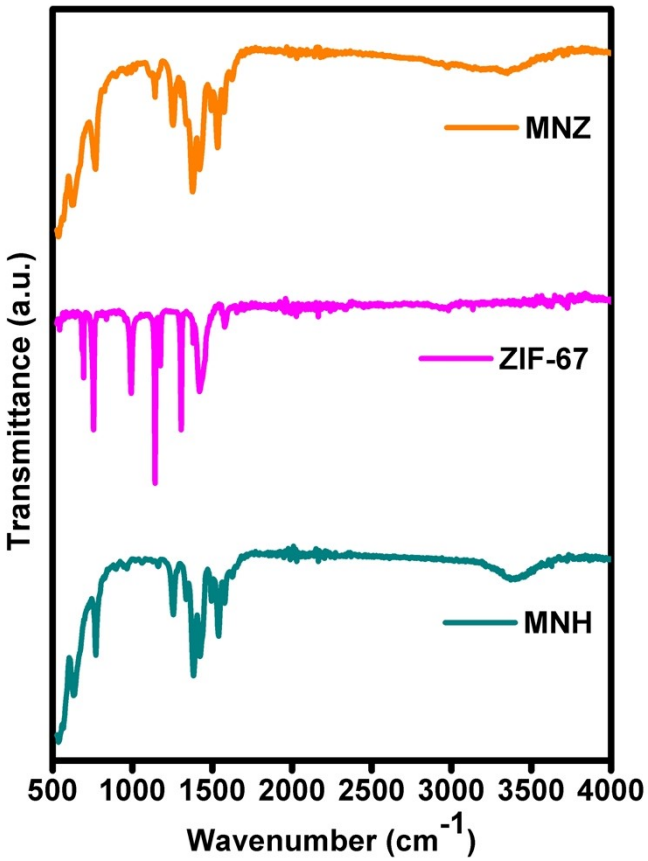

Fig. S1. FT-IR spectra of the prepared photocatalysts.

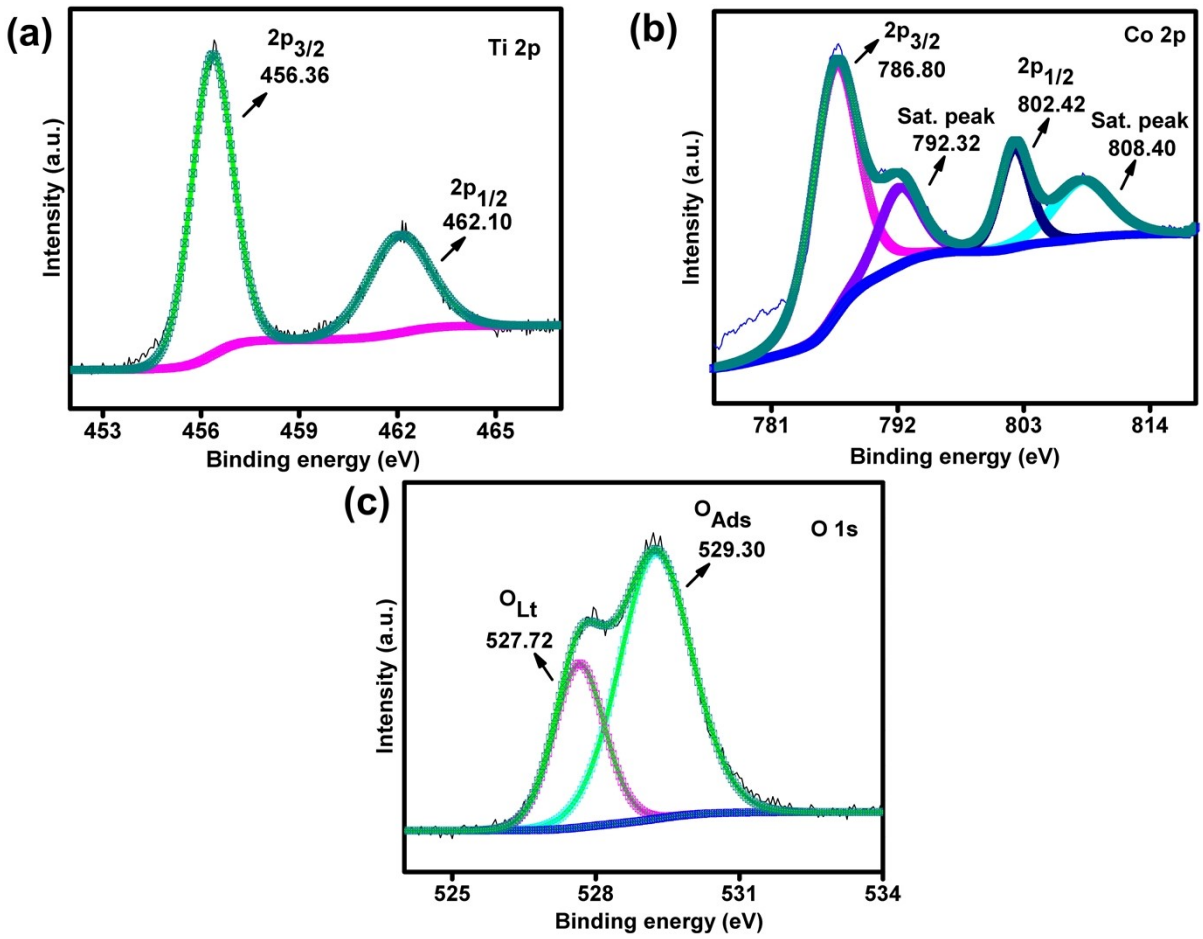

Fig. S2. XPS spectra of (a) MNH Ti 2p, (b) ZIF-67 Co 2p, (c) MNH O 1s.

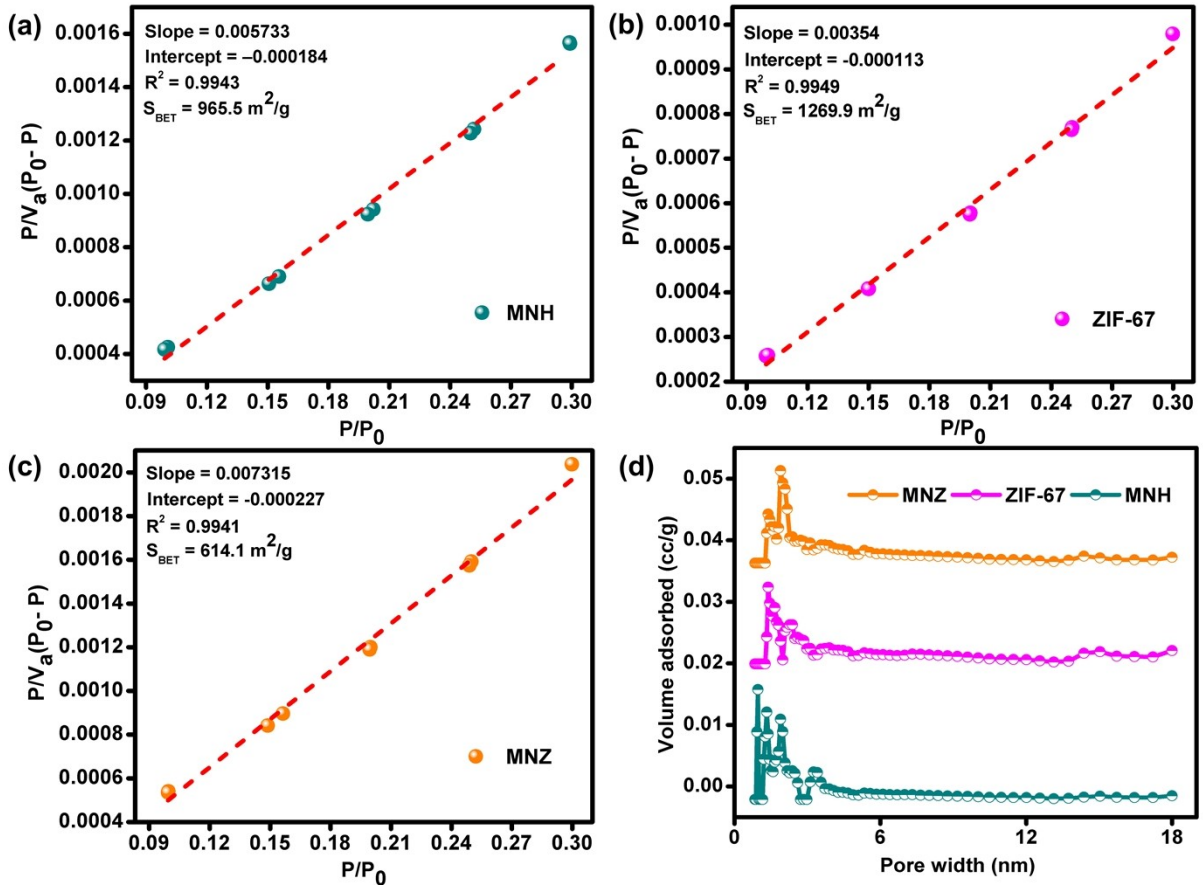

Fig. S3. Linear BET plot of (a) MNH, (b) ZIF-67, and (c) MNZ. (d) Pore size distribution plot of the photocatalysts.

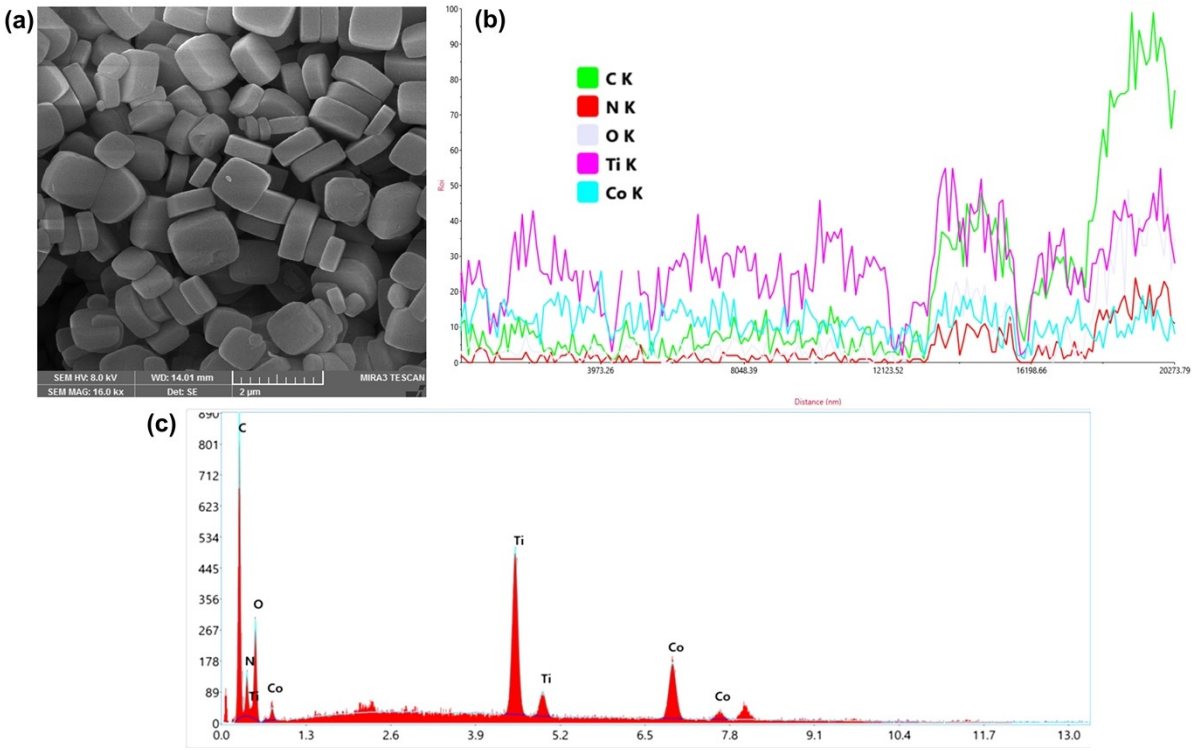

Fig. S4. (a) FESEM image of MNH. (b) Element profile plot of MNZ. (c) EDX elemental mapping analysis of MNZ.

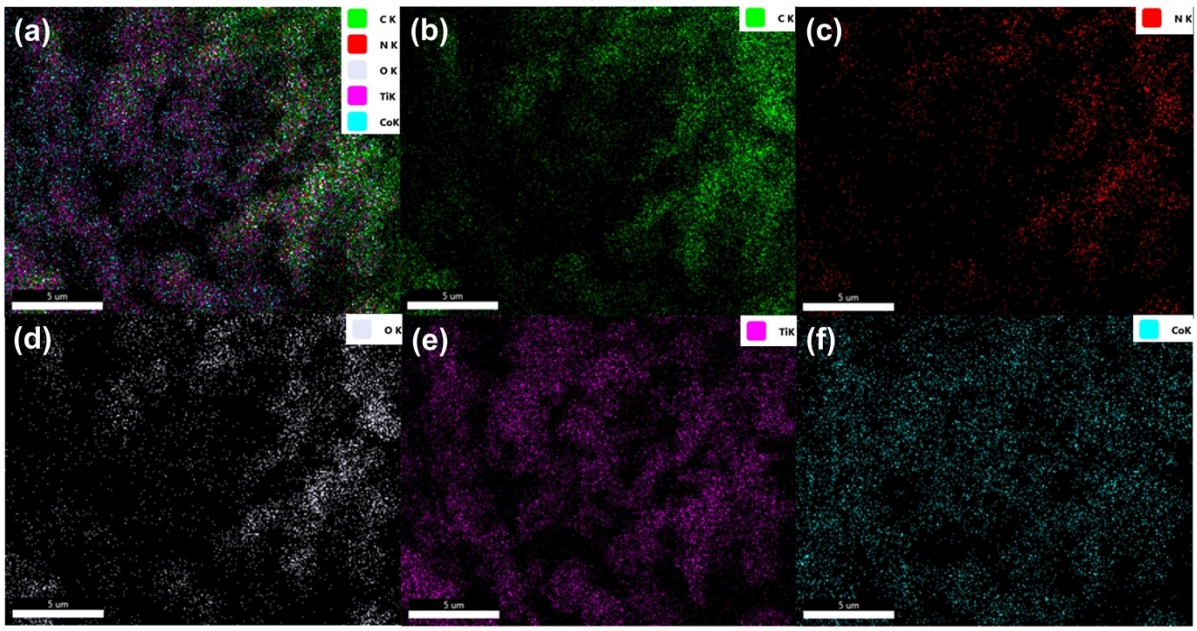

Fig. S5. Layered EDX mapping showing the elemental distribution in the MNZ composite.

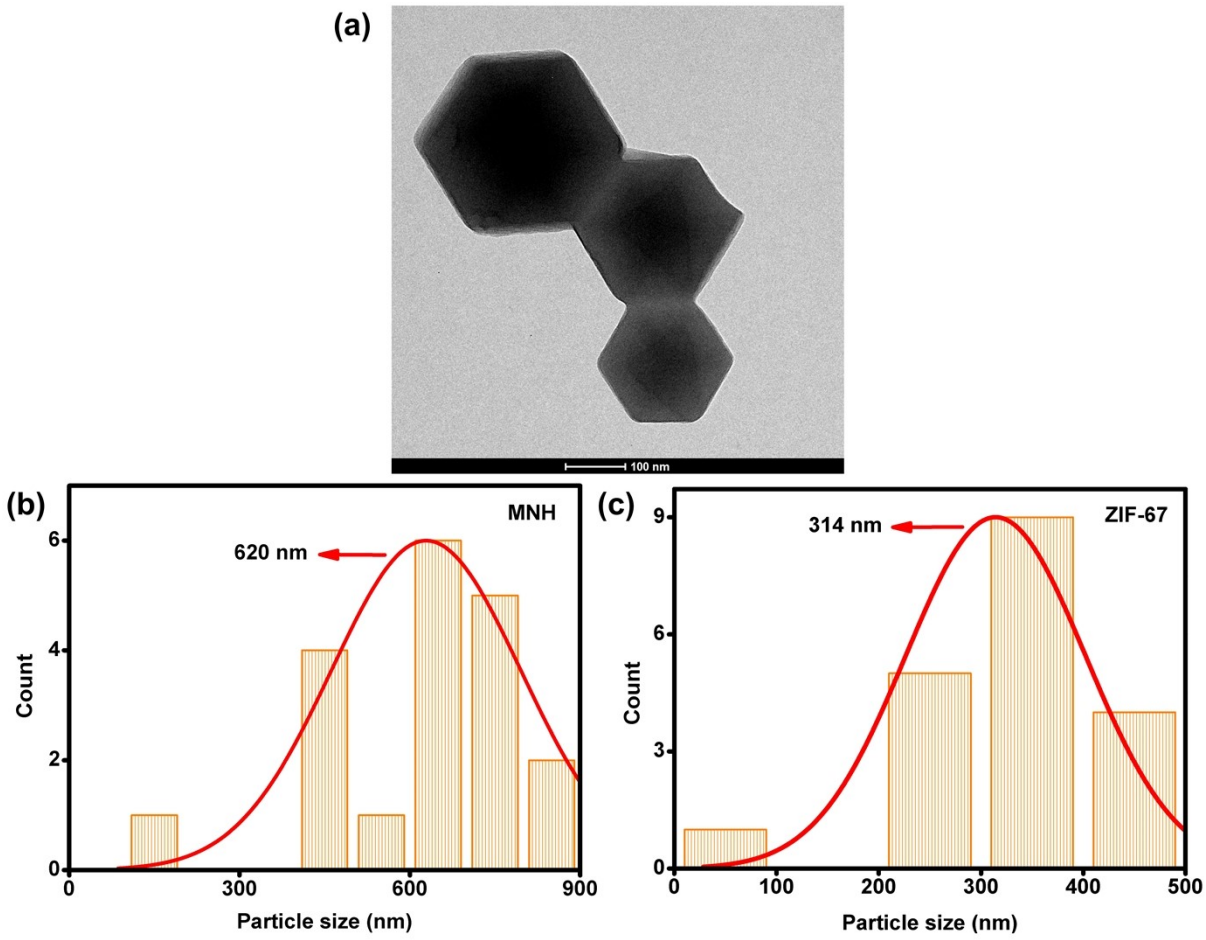

Fig. S6. (a) HRTEM image of ZIF-67. Particle size distribution histogram of (b) MNH and (c) ZIF-67.

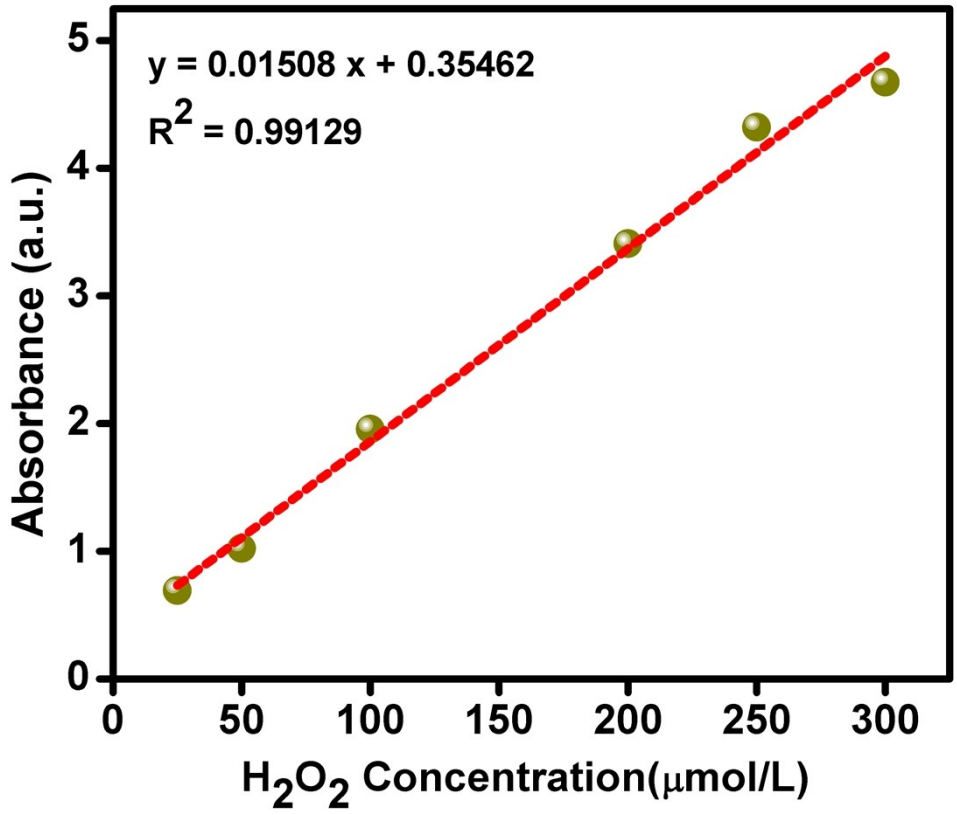

Fig. S7. Standard curve of H_2O_2 measured by iodimetry.

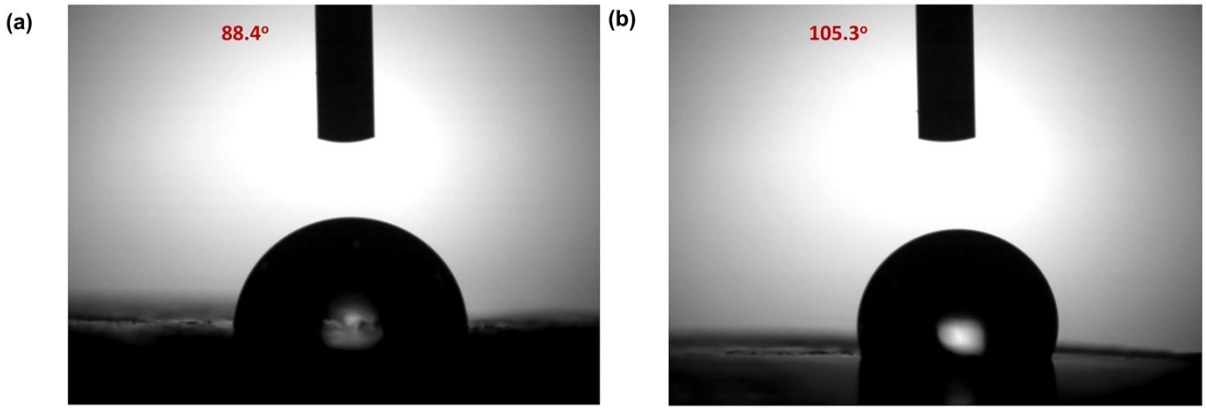

Fig. S8. Contact angle measurement of (a) MNH and (b) MNZ.

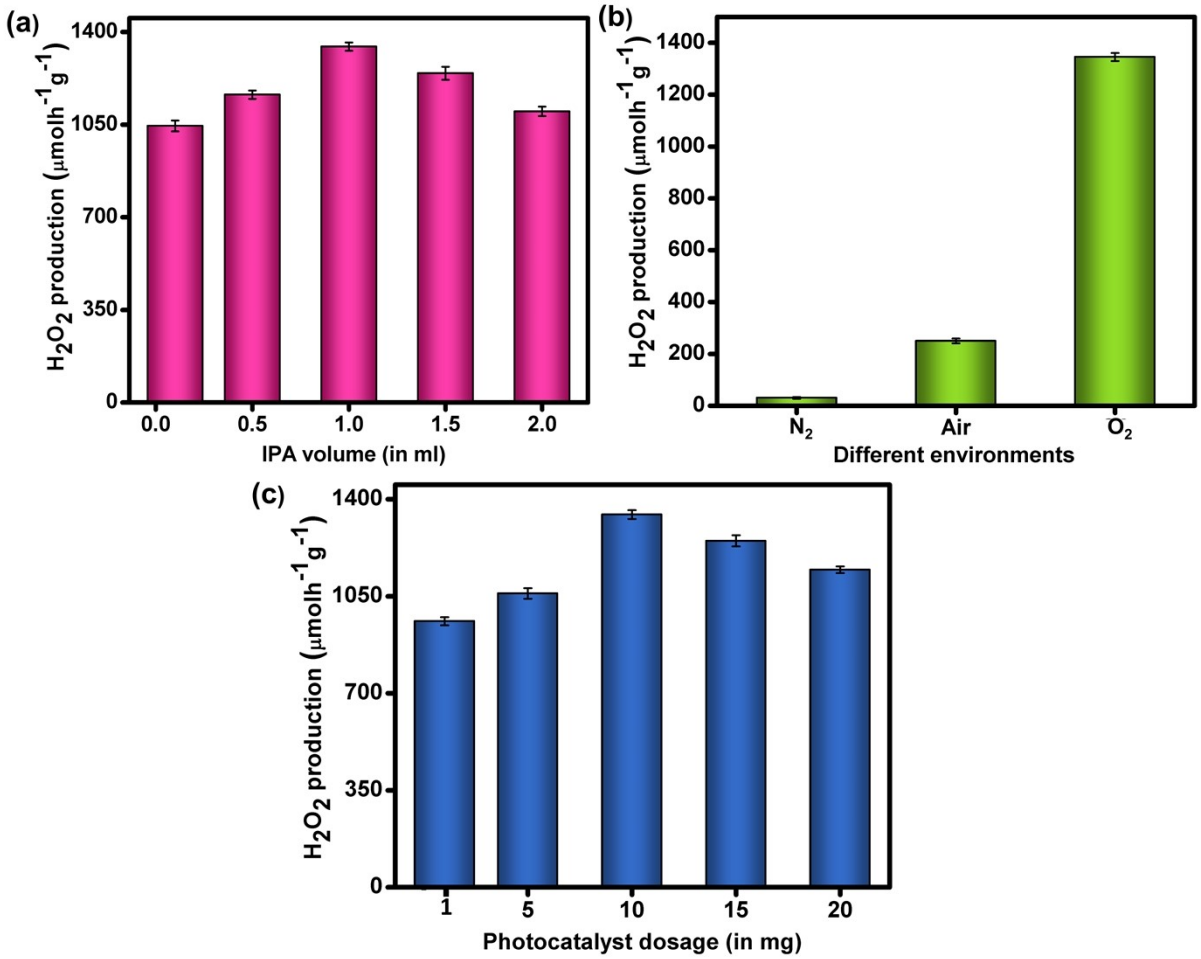

Fig. S9. (a) Effect of IPA concentration on H_2O_2 generation. (b) Impact of O_2-saturated conditions on photocatalytic performance. (c) Influence of photocatalyst dosage on H_2O_2 production efficiency. Error bars represent mean ± SD of three independent measurements.

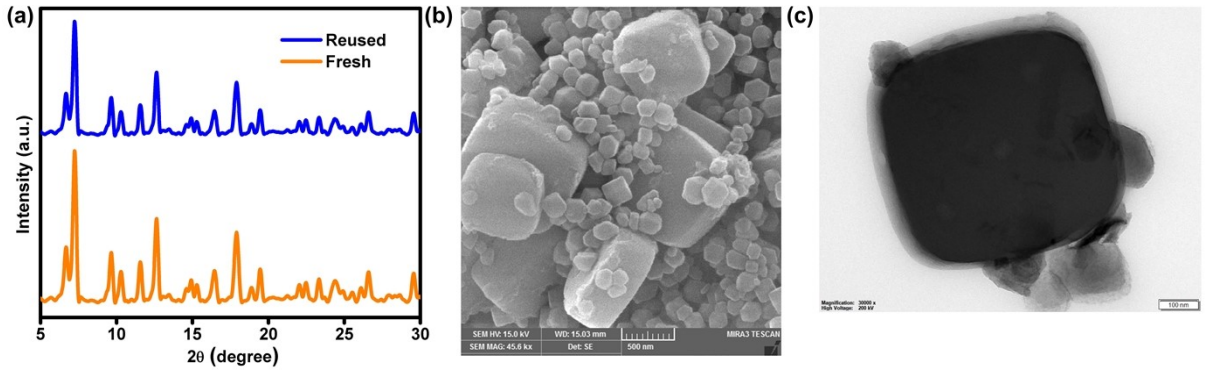

Fig. S10. Post-reaction (a) PXRD, (b) FESEM image, (c) HRTEM image of MNZ.

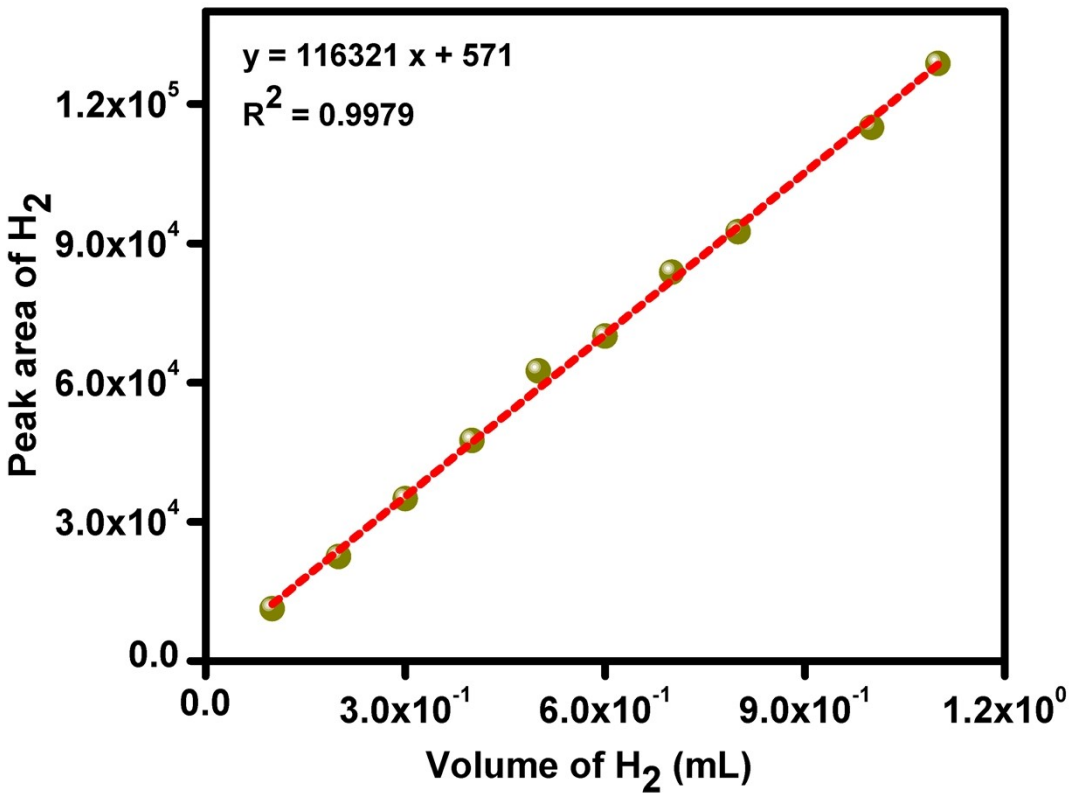

Fig. S11. The calibration plot for H_2, as tested using gas chromatography.

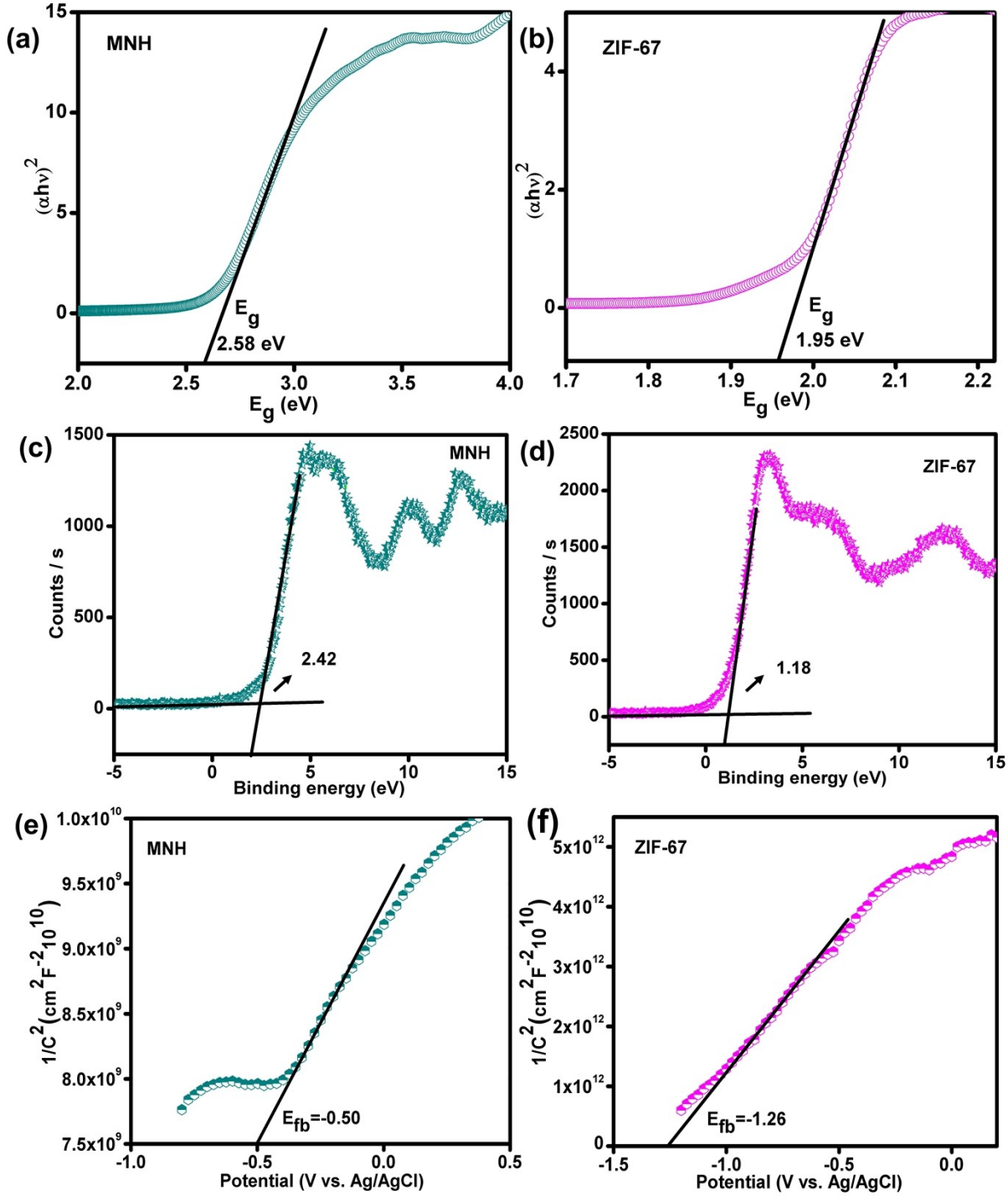

Fig. S12. Tauc plot of (a) MNH, (b) ZIF-67. XPS valence band spectra of (c) MNH and (d) ZIF-67. Mott−Schottky plot for (e) MNH and (f) ZIF-67.

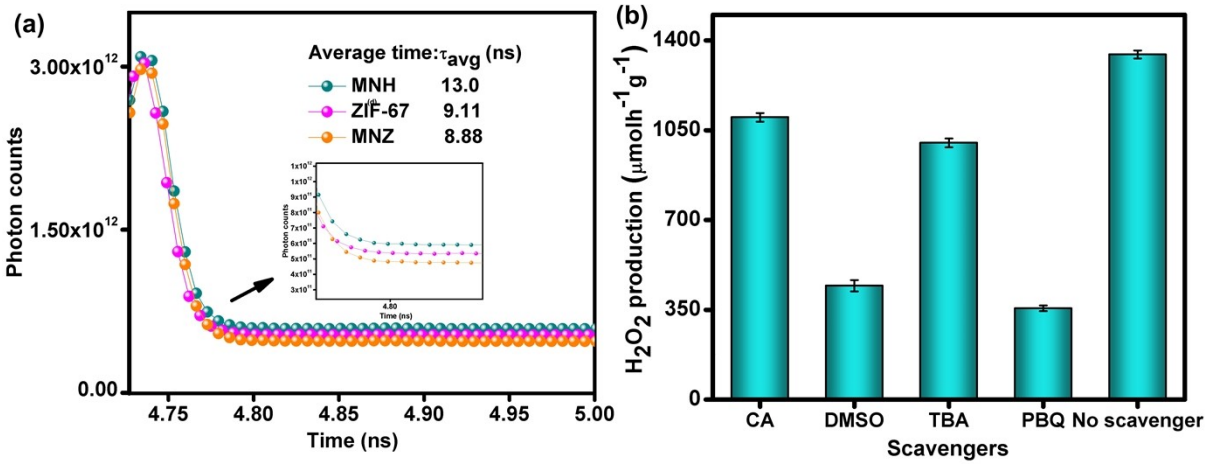

Fig. S13. (a) TRPL spectra of the photocatalyst. (b) H_2O_2 generation rate under different reactive species scavengers. Error bars represent mean ± SD of three independent measurements.

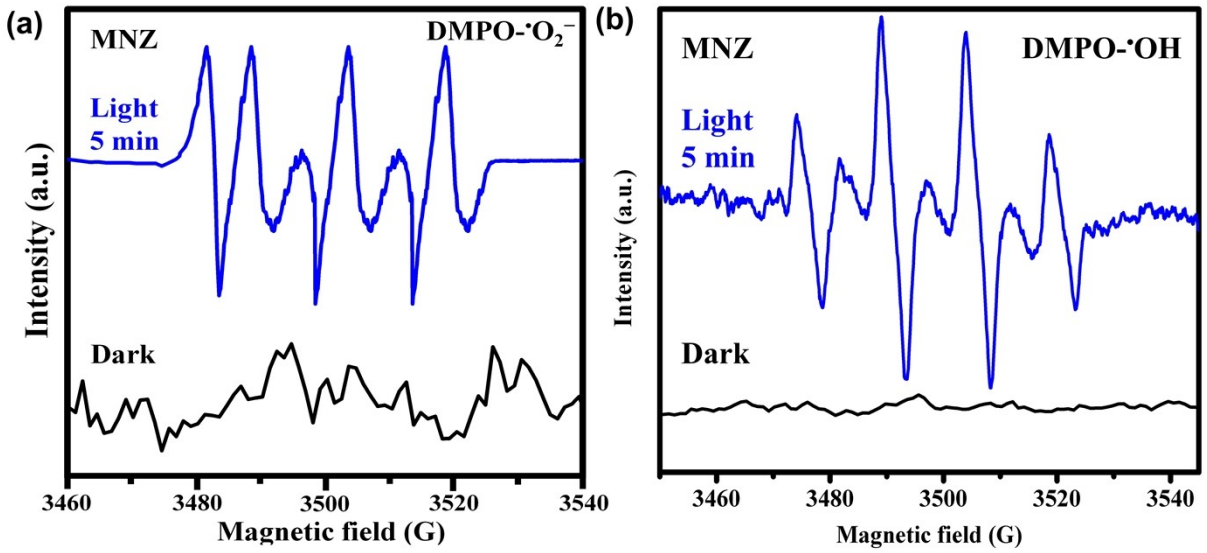

Fig. S14. ESR spectra under dark and visible-light conditions for (a) superoxide ($•O_2^-$) and (b) hydroxyl (•OH) radicals.

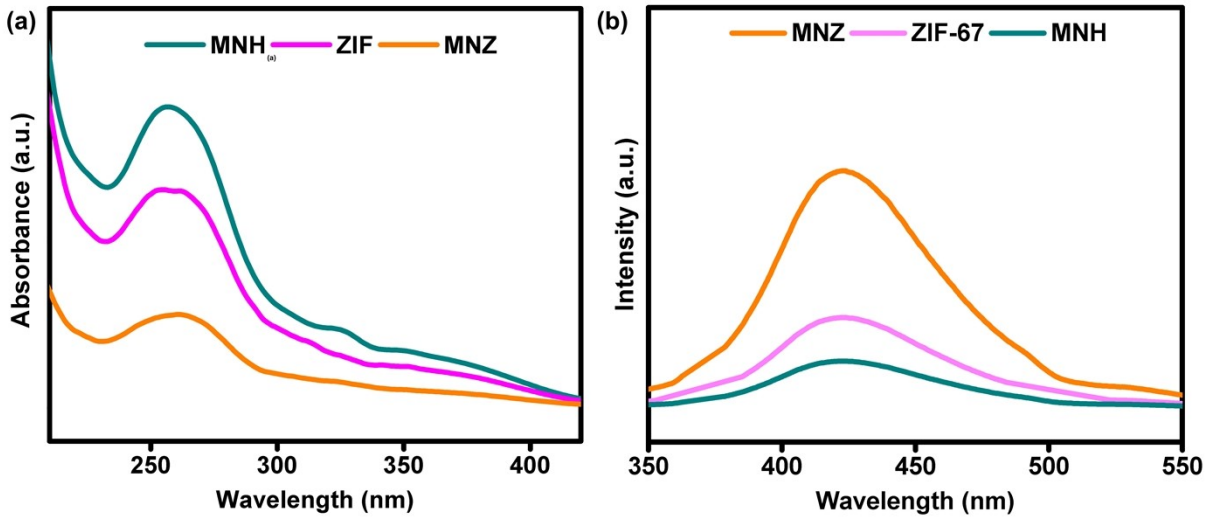

Fig. S15. (a) NBT assay and (b) TA fluorescence test results for MNH, ZIF-67, and MNZ.

Table S1. BET surface area and pore volume of MNH, MZ, and MNZ photocatalysts.

Photocatalyst	**Calculated S_{BET} (m^2/g)**	**Instrument S_{BET} (m^2/g)**	**Pore diameter (nm)**	**Pore volume (cm^3/g)**
MNH	965.5	981.38	4.8	0.40
ZIF-67	1269.9	1265.30	3.05	0.007
MNZ	614.4	589.30	6.78	0.26

Table S2. Calculated AQE values of the MNZ photocatalyst at various bandpass filters.

$\lambda_{bandpass\ (nm)}$	**AQE (%)**
340	2.00
400	3.64
450	1.07
500	0.43
550	2.72

Table S3. Calculated SCC% values of the as-prepared photocatalysts.

	MNH	**ZIF-67**	**MNZ**
SCC%	0.0130	0.0138	0.025

Table S4. Calculated ACE% values of the as-prepared photocatalysts.

	MNH	**ZIF-67**	**MNZ**
ACE%	1.28	1.49	3.45